Reducing the sensitivity of semiconductor ring lasers to external optical injection using selective optical feedback

Khoder, Mulham; Van Der Sande, Guy; Verschaffelt, Guy

Published in:
Journal of Applied Physics

DOI:
10.1063/1.5046073

Publication date:
2018

Reducing the sensitivity of semiconductor ring lasers to external optical injection using selective optical feedback

Mulham Khoder, Guy Van der Sande, and Guy Verschaffelt

Citation: Journal of Applied Physics **124**, 133101 (2018); doi: 10.1063/1.5046073
View online: https://doi.org/10.1063/1.5046073
View Table of Contents: http://aip.scitation.org/toc/jap/124/13
Published by the American Institute of Physics

Reducing the sensitivity of semiconductor ring lasers to external optical injection using selective optical feedback

Mulham Khoder,[1,a)] Guy Van der Sande,[2] and Guy Verschaffelt[2]
[1]*Brussels Photonics (B-PHOT), Department of Applied Physics and Photonics, Vrije Universiteit Brussel, Pleinlaan 2, B-1050 Brussels, Belgium*
[2]*Applied Physics Research Group (APHY), Department of Applied Physics and Photonics, Vrije Universiteit Brussel, Pleinlaan 2, B-1050 Brussels, Belgium*

(Received 25 June 2018; accepted 10 September 2018; published online 1 October 2018)

We numerically investigate the influence of an integrated filtered optical feedback on the behavior of a semiconductor ring laser subject to external optical injection. The optical injection is spectrally directed at one of the non-lasing longitudinal modes of the laser. This so-called side-mode injection can cause wavelength switching, directional switching, and changes in the dynamical regime of the semiconductor ring laser. Such changes are often unwanted as they can affect the stability and the performance of the semiconductor ring laser. We investigate to what extent these undesired effects can be avoided by stabilizing the laser using on-chip filtered feedback. A two-directional mode model is used to investigate the dynamical behavior of the semiconductor ring laser under the simultaneous effect of the external optical injection and the integrated feedback. The results show that on-chip filtered optical feedback can be used to reduce the sensitivity of the semiconductor ring laser to external optical injection. *Published by AIP Publishing.* https://doi.org/10.1063/1.5046073

I. INTRODUCTION

It is well known that semiconductor lasers are very sensitive to external optical injection (OI).[1] OI can be useful for mode locking,[2] linewidth narrowing and chirp reduction,[3] cryptographic applications,[4] and for optical switching applications.[5]

The frequency of the injected signal of the master laser (ML) can be close to the frequency of the free-running lasing mode of the slave laser (SL) to achieve what is called intramodal injection locking. This intramodal injection has been used, e.g., to enhance the modulation bandwidth of semiconductor lasers.[6–8] Another type of optical injection is called sidemode (intermodal) injection which occurs when the light of the ML is injected close to a nonlasing longitudinal sidemode. This type of optical injection has been used to measure the semiconductor laser gain spectra[9] and to enhance the stable locking range.[10]

Sometimes, a part of light of one laser is coupled unintentionally to a second laser. This undesired injection can be difficult to avoid in integrated optical networks with many different semiconductor lasers all placed on the same chip. It can happen that light from one integrated laser is slightly reflected or scattered from other integrated components. The light can then follow an unexpected path through the optical network and be coupled to another integrated laser. This undesired injection can then change the operating wavelength of this second laser or even destabilise its behavior.[11,12] As a result, the entire operation of the optical chip can be compromised.

One way to avoid these effects of OI is by using an optical isolator. Several approaches have been proposed to achieve on-chip isolation.[13–15] However, such isolators introduce an additional cost and implementing them can be challenging[16,17] as the on-chip integration of magneto-optic materials, needed to make an optical isolator, is difficult.

Another approach that has been suggested to control the output of semiconductor lasers and to make them less sensitive to external perturbations is the use of filtered optical feedback.[18] In that case, only short feedback lengths are needed, which makes it possible to integrate the filtered feedback on the laser chip resulting in a compact and low-cost approach. Such an integrated optical feedback (IOF) has, for example, been used to tune the emission wavelength of Fabry-Perot lasers:[19] a particular longitudinal mode can be selected for lasing by controlling the strength and the phase of the IOF.

Recently, semiconductor ring lasers (SRLs) have attracted considerable interest as laser sources in photonic integrated circuits. These lasers can support lasing in the clockwise (CW) and counterclockwise (CCW) propagating modes and it is possible to achieve switching between the two directions.[20] This makes SRLs interesting for some applications as optical memories[21] and random numbers generators.[22] But these SRLs are—similar to other semiconductor lasers—very sensitive to optical injection,[23–25] and therefore it is interesting to investigate schemes that can reduce this sensitivity. Using filtered optical feedback can possibly achieve this goal and is investigated in detail in this work.

Optical feedback can be integrated with SRLs following different interconnection schemes, which are illustrated in Fig. 1. Figure 1(a) shows a schematic of the SRL, while Fig. 1(b) illustrates the cross-feedback interconnection scheme: part of the light emitted by the SRL in the CCW direction is coupled back to the SRL in the CW direction. Remark that it is of course also possible to implement a

a)Electronic mail: mulham.khoder@vub.be

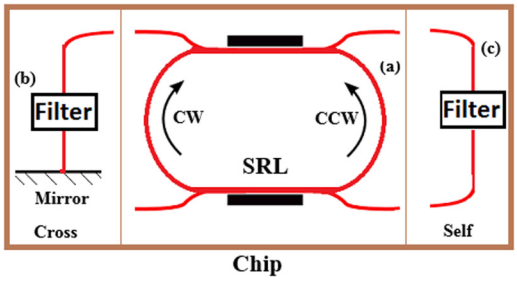

FIG. 1. (a) Schematic of an integrated SRL with (b) cross and single IOF using a short waveguide, (c) self and double IOF using a short waveguide.

cross-feedback configuration in which we couple the CW mode to the CCW mode. In Fig. 1(c), we schematically illustrate the self-feedback scheme in which the CW and CCW modes are coupled to themselves after passing the IOF path. The delay time of the IOF paths can be designed anywhere between approximately a few tens of picoseconds up to several nanoseconds.[26] These limits are imposed on the one hand by the minimum physical size of the different components in the IOF path (such as splitters, filters, semiconductor optical amplifiers (SOAs), and mirrors) and on the other hand by the on-chip waveguide losses. Here, we will focus on short IOF delay lengths because long feedback lengths are prone to destabilize the laser by introducing delay dynamics.[27] The filter in Figs. 1(b) and 1(c) gives the IOF its selectivity as it allows the feedback to tune the wavelength of the SRL. The filtering process can be achieved using distributed Bragg reflector mirror (DBR)[28] or using arrayed waveguide gratings (AWGs).[29]

An example of an SRL with single cross and filtered feedback is discussed in Ref. 28, where a monolithically integrated external DBR has been used to provide an IOF tuning mechanism for the SRL wavelength. The wavelength of the IOF is controlled by changing the reflectivity of the DBR. The phase and the strength of the feedback are controlled using a phase section and a semiconductor optical amplifier, respectively. The results have shown single mode emission with a side mode suppression ratio of 30 dB. An integrated SRL with double and self (filtered) feedback has been introduced in Ref. 29. In this device, the IOF section consists of two AWGs which are mutually connected via four SOAs gates. The phase and the strength of the feedback can be controlled using SOA gates. This device has been used to demonstrate digital wavelength tuning and multi-wavelength laser emission.[30–33]

In this paper, we investigate an approach to reduce the undesired effects of external OI on SRLs using on-chip feedback. We use a two-directional mode rate equation model to investigate the output of the SRL under the simultaneous effect of the filtered IOF and OI. We show that the output of the SRL is determined according to a competition between the longitudinal mode (LM) which is enhanced by the OI and the LM which is enhanced by IOF. We show that using a sufficiently strong IOF, it is possible to reduce several effects of the external OI. For example, the minimum injection strength required for wavelength and directional switching is increased when increasing the IOF strength. This can be achieved without the need for any external bulky isolators[16] or on-chip isolation[34] which are normally used to avoid OI-induced dynamics. We also investigate the role of other laser, OI, and IOF parameters, such as the phase and strength of the IOF and the strength of the OI.

The remainder of the paper is organized as follows. In Sec. II, we present the model equations describing the SRL, the IOF, and the OI. Section III is devoted to showing the effect of IOF on the SRL. In Sec. IV, the SRL is investigated under the simultaneous effect of IOF and OI. At the end of the paper, some conclusions are drawn.

II. THEORETICAL MODEL

Several models have been proposed to analyze the dynamical features of SRLs. These models describe the interplay between the two counter-propagating modes and their effect on the gain medium. In Ref. 35, Sargent suggested a rate equation model using the intensities of the two modes taking into account the effect of both self- and cross-saturation. Another model has been derived by Etrich *et al.* using the electric field in the two directions.[36] A traveling wave model for SRLs with optical feedback has been proposed by Radziunas.[37] An asymptotic two-dimensional model has been used to describe the dynamical behavior of SRLs in Ref. 38. In this work, we use a two-directional mode rate equation model which takes into account the effects of backscattering and gain saturation.[39,40] The evolution of the electric fields and the carriers are described by the following equations for two LMs:

$$\dot{E}_1^{cw} = \kappa(1+i\alpha)\left[NG_1^{cw}-1\right]E_1^{cw} - \left(k_d + ik_c^{ccw}\right)E_1^{ccw} + \eta_1 E_1^{cw}(t-\tau)e^{i\theta_1} - i\triangle E_1^{cw}, \tag{1}$$

$$\dot{E}_1^{ccw} = \kappa(1+i\alpha)\left[NG_1^{cw}-1\right]E_1^{ccw} - \left(k_d + ik_c^{cw}\right)E_1^{cw} + \eta_1 E_1^{ccw}(t-\tau)e^{i\theta_1} - i\triangle E_1^{ccw} + \frac{1}{\tau_{in}}E_1^{i}, \tag{2}$$

$$\dot{E}_2^{cw} = \kappa(1+i\alpha)\left[NG_2^{cw}-1\right]E_2^{cw} - \left(k_d + ik_c^{ccw}\right)E_2^{ccw} + \eta_2 E_2^{cw}(t-\tau)e^{i\theta_2}, \tag{3}$$

$$\dot{E}_2^{ccw} = \kappa(1+i\alpha)\left[NG_2^{cw}-1\right]E_2^{ccw} - \left(k_d + ik_c^{cw}\right)E_2^{cw} + \eta_2 E_2^{ccw}(t-\tau)e^{i\theta_2}, \tag{4}$$

$$\frac{1}{\gamma}\dot{N} = \mu - N - N\sum_{m=1}^{n=2}\left(G_m^{cw}|E_m^{cw}|^2 + G_m^{ccw}|E_m^{ccw}|^2\right). \tag{5}$$

The symbols $E_{1,2}^{cw}$ and $E_{1,2}^{ccw}$ indicate the normalized counter-propagating fields for LM_1 and LM_2, κ is the field decay rate, α is the linewidth enhancement factor, γ is the carrier inversion decay rate, k_d and k_c are dissipative and conservative scattering coefficients, and μ is the normalized injection current. The laser threshold condition corresponds to μ=1. G_m^{cw} and G_m^{ccw} are the differential gain functions for $m = 1, 2$.

which are given by

$$G_m^{cw} = \left(1 - S|E_m^{cw}|^2 - C|E_m^{ccw}|^2\right), \tag{6}$$

$$G_m^{ccw} = \left(1 - S|E_m^{ccw}|^2 - C|E_m^{cw}|^2\right). \tag{7}$$

Here S and C are normalized self and cross gain saturation coefficients. The subscript "m" is used to identify different LMs while n represents the total number of LMs. In our study, we only consider two LMs. We use Lang-Kobayashi terms to include the IOF in the model,[41] by representing the strength and the phase of the filtered IOF which are applied to mode "m" by η_m and θ_m, respectively. τ is the propagation time in the integrated feedback section. Similar to the models in Refs. 18, 29, and 33, where the SRLs have mode spacing around 0.3 nm, we neglect gain saturation between the LMs as it is expected to be small because the LMs have different wavelengths. The LMs are thus only coupled through their common carrier reservoir. In the general case, LM1 and LM2 will not be adjacent LMs and their spectral separation will be several times larger than 0.3 nm. Such a large spacing will typically lead to negligible spectral and spatial hole burning.

The parameters of the OI are τ_{in}, which is the cavity round-trip time, $E_1^i > 0$, which is the injected field amplitude, and $\triangle$, which is the spectral detuning between the optical frequency of the injected signal and the optical frequency of the LM of the SRL. A detuning $\triangle > 0$ corresponds to a higher frequency of the injected signal than the SRL.[9,25] As LM1 and LM2 are well-separated, they only interact incoherently via the carrier reservoir. This makes the inclusion of a detuning in the equations of LM_2 unnecessary.

We choose the IOF in this work to be double and self feedback, i.e., the CW (CCW) mode is coupled by the IOF to the CW (CCW) mode. Furthermore, the IOF has been chosen to be wavelength selective feedback such that it can be used to favor a particular LM. In Ref. 29, such an IOF scheme has been fabricated on the same chip as the SRL. It has been shown experimentally that IOF can tune the emission wavelength of the SRL. We choose to inject the external optical signal in the CCW direction and close to LM_1.

TABLE I. Parameter values of a SRL subject to IOF.

Parameter	Symbol	Value
Linewidth enhancement factor	α	3.5
Self-saturation coefficient	S	0.005
Cross-saturation coefficient	C	0.01
Dissipative bacskcattering	k_d	$0.2\,ns^{-1}$
Conservative bacskcattering CW	k_c^{cw}	$0.88\,ns^{-1}$
Conservative bacskcattering CCW	k_c^{ccw}	$1.144\,ns^{-1}$
Photon lifetime	τ_{ph}	$5\,ps$
Carrier inversion decay rate.	γ	$0.2\,ns^{-1}$
Renormalized injection current	μ	1.2
Field decay rate	κ	$200\,ns^{-1}$
The delay time of the IOF	τ	$75\,ps$
Cavity round-trip time	τ_{in}	$26.5\,ps$
Number of the simulated LMs	n	2
Strength of IOF	η_m	var
Phase of IOF	θ_m	var

III. SRL SUBJECT TO IOF

We start by showing the effect of the IOF on the output of the SRL without any OI. We study the effect of the strength and the phase of the IOF using Eqs. (1)–(5) and by considering two LMs ($n = 2$) and by setting the OI parameters to zero ($E_1^i = \triangle = 0$).

A small asymmetry between the two directional modes is introduced via the conservative backscattering coefficients in order to allow us to distinguish between the LMs in the CW and CCW directions. The values of these coefficients (see Table I) have been chosen equal to the values in Refs. 18, 29, and 30 which are estimated based on experimental results. The delay time of the IOF was chosen to be $\tau = 75\ ps$. The delay line corresponding to this delay time can easily be integrated on a chip using waveguides. Similar delay lines have been fabricated and characterized in Refs. 28, 29, and 42, and they are offered by several foundries via the Jeppix platform.[43] We choose one of the two modes (LM_2) to be supported by feedback while LM_1 is without feedback by setting $\eta_1 = \theta_1 = 0$. The values of the other parameters are given in Table I.

A. Effect of the strength of IOF

We calculate the intensities of LM_1 and LM_2 in the CW and the CCW directions when the feedback strength of LM_2 is increased from 0 to 15 ns^{-1} while $\theta_2 = \pi/2$, i.e., we investigate the SRL's behavior when the feedback light arrives back at the SRL with a shifted phase as compared to the original beam phase. We choose this value of the phase (0.5π) as it is in the middle of the two extreme values which are the in phase value ($\theta_2 = 0$) and the anti-phase value ($\theta_2 = \pi$).

As can be seen in Fig. 2, when $\eta_2 = 0$ ns^{-1} both LM_1 and LM_2 have the same intensity in the CW direction and in the CCW direction, and the SRL's output is multi-mode. The difference in the intensity between the CW and the CCW direction is due to the introduced asymmetry in the backscattering coefficients. By increasing η_2, we notice that the intensity of LM_2 increases in the two directions while the intensity of LM_1 decreases in the two directions. When η_2 is larger than 3 ns^{-1}, LM_2 dominates while LM_1 is switched

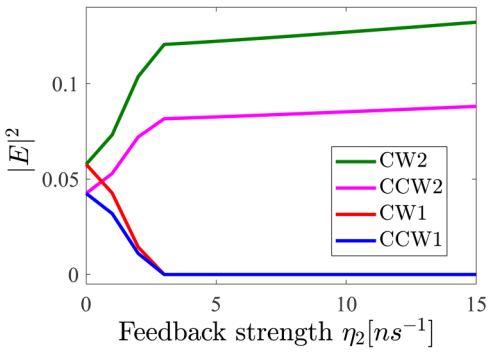

FIG. 2. $|E|^2$ as a function of the strength of IOF while the other parameters are $\mu = 1.2$, $\eta_1 = \theta_1 = 0$, $\theta_2 = \pi/2$, and τ=75 ps.

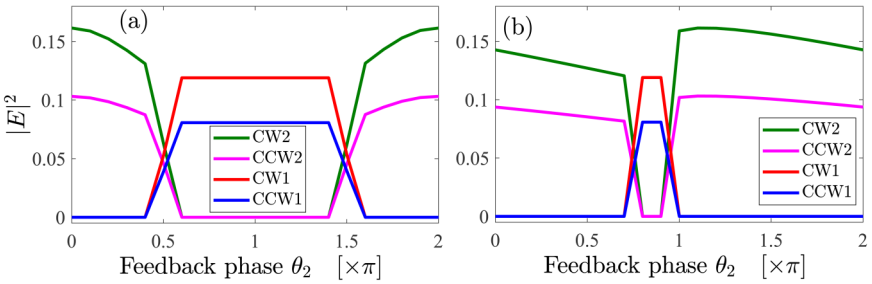

FIG. 3. $|E|^2$ as a function of the feedback phase while the other parameters are $\mu = 1.2$, $\eta_1 = \theta_1 = 0$, $\eta_2 = 10\,\mathrm{ns}^{-1}$. (a) $\tau = 0$ ps, (b) $\tau = 75$ ps.

off. From Fig. 2, it is clear that by using IOF it is possible to enhance a specific LM in order for it to dominate the output of the SRL.

B. Effect of the phase of IOF

We also investigate the effect of the phase of the IOF by applying feedback to one of the two LMs. We choose LM_2 to be supported by IOF while LM_1 is without feedback by setting $\eta_2 = \theta_2 = 0$. In our first calculations, we neglect the delay of the IOF by setting τ to zero. This is not entirely correct as the feedback delay of IOF is 75 ps, but we start with this case to investigate the effect of the phase without considering the effect of (the phase of) any external cavity mode (ECM) which can appear due to the delay. We plot the intensity of both $LM_1$and LM_2 in the CW and the CCW directions while we increase the feedback phase of LM_2 from 0 to 2π. The feedback strength during these calculations is fixed to $\eta_2 = 10\,ns^{-1}$ while $\eta_1 = 0\,ns^{-1}$. As can be seen in Fig. 3(a), when θ_2 is in the range [0–π], LM_2 is dominant for $\theta_2 < 0.5\pi$, whereas $\theta_2 > 0.5\pi$ results in LM_2 being gradually switched off. When θ_2 is in the range [π–2π], LM_2 is switched off for $\theta_2 < 1.5\pi$, whereas $\theta_2 > 1.5\pi$ results in LM_2 being gradually increased. When θ_2 is in the range [1.6π–2π], LM_2 is dominant while LM_1 is off.

Next, we repeat the calculations but this time by considering a realistic value of the delay time of the on-chip feedback loop ($\tau = 75$ ps). As we can see in Fig. 3(b), when θ_2 is in the range [0–π], LM_2 is dominant for $\theta_2 < 0.75\pi$, whereas $\theta_2 > 0.75\pi$ result in LM_2 being gradually switched off. LM_2 is switched off when θ_2 is in the range [π–2π]. These results are similar to the results in Fig. 3(a) but the ranges of θ_2 where LM_2 is dominant have expanded on the expense of the ranges where LM_2 is dominant. These changes can be understood as being due to the appearance of so-called external cavity modes (ECMs) because of the finite value of the delay.[44] These are single frequency steady state solutions of Eqs. (1)–(5).

These ECMs are typically created in pairs when the feedback strength increases. Each of the ECMs will have a (slightly) different wavelength. The SRL with IOF can thus select that ECM whose feedback phase is closest to zero. Therefore, the regions of LM_1 (or LM_2) being selected in Fig. 3(b) will be somewhat different from those in Fig. 3(a), and these regions can further shift if we change the feedback delay time.

Here, it is important to note that the general conclusion still holds: either LM_1 or LM_2 can be selected by changing the feedback strength and/or phase of one of the LMs. By considering the effect of the phase and the strength of the IOF, we can conclude that the effective strength of the selected mode by IOF depends on both the strength and the phase of IOF. This also shows that IOF can efficiently be used to select a specific LM to dominate the output of the SRL.

IV. SRL SUBJECT TO IOF AND OI SIMULTANEOUSLY

In this section, we investigate the laser's output under the effect of both the IOF and OI at the same time. As in Sec. III, we have limited the number of LMs to two ($n = 2$) as it corresponds to the minimum number of modes which is needed to describe the wavelength change due to the OI.

The injected signal can be injected either close to the free-running laser mode or close to one of side modes.[47] A theoretical study about an SRL with OI close to the peak lasing mode has been discussed in Ref. 25 Here, we investigate the SRL subject to light which is injected close to a side mode (LM_1). This injected signal clearly has a different frequency from the lasing mode (LM_2) as can be seen in Fig. 4. The IOF enhances LM_2 which thus will be the lasing mode of the SRL when no OI is applied as discussed in Sec. III. To clarify the alignment between the LMs of the SRL and the injected signal, we show the scheme in Fig. 4 where the OI targets a side mode (LM_1). We do not specify which side-mode is targeted by the OI. As we assume that the gain saturation between the LMs is small, the results will not depend on the actual wavelength difference between LM_1 and the lasing mode LM_2.

First, we show the effect of OI without applying IOF. We choose the cavity round-trip time in our calculations to be $\tau_{in} = 26.5$ ps which is similar to the value of the cavity round-trip in Refs. 28, 29, and 42. The detuning between the injected signal and LM_1 chosen in this example is $\triangle = -2\,ns^{-1}$. In Figs. 5(a) and 5(b), we show the orbit diagrams for both LMs and for both directions as a function of the injection signal amplitude E_1^i. When no signal is injected in LM_1 (i.e., $E_1^i = 0$), the intensity of both LMs is equal while the intensity in the CW direction is somewhat larger

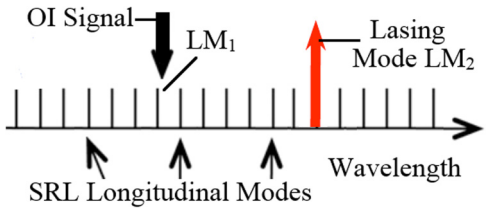

FIG. 4. The alignment between the LMs of the SRL and the OI signal.

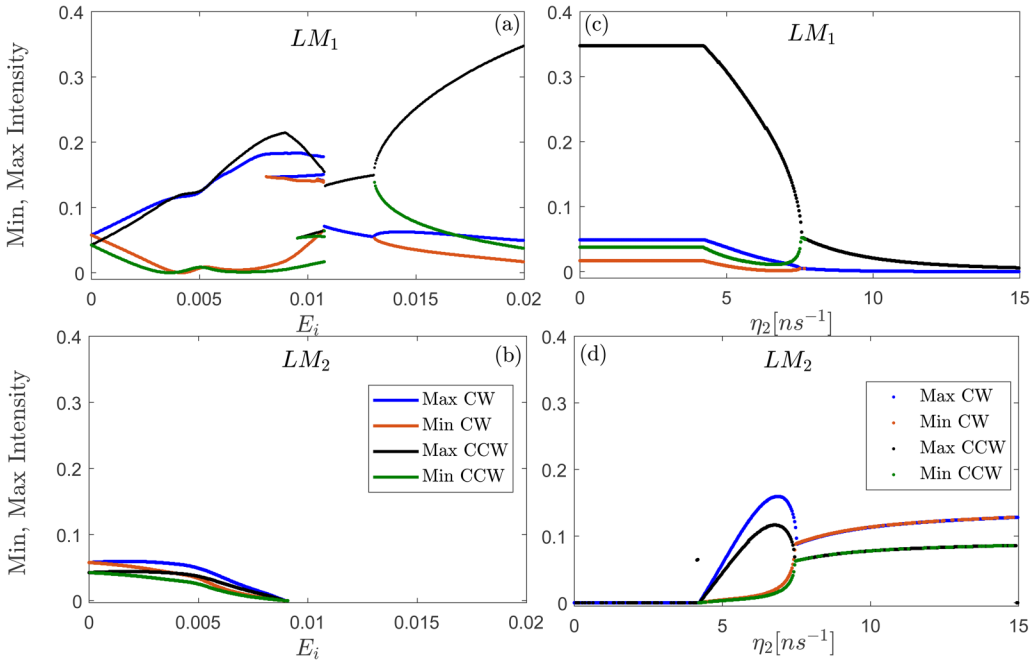

FIG. 5. Orbit diagrams showing the maxima and minima in time-traces [simulated using Eqs. (1)–(5)] [(a), (b)] for different values of the injection amplitude E_1^i while $\triangle = -2\,ns^{-1}$, $\eta_1 = \eta_2 = 0\,ns^{-1}$ and [(c), (d)] for different values of the IOF strength η_2 while $\triangle = -2\,ns^{-1}$, $E_1^i = 0.02$, $\eta_1 = 0\,ns^{-1}$, and $\theta_2 = 0.5\pi$.

than in the CCW direction, very similar to the situation in Fig. 2(a) at a feedback strength close to zero. When we increase E_1^i, we observe periodic oscillations in the time traces as is evidenced by the single maximum and single minimum in the orbit diagram at small values of E_1^i. The angular frequency of these oscillations is approximately equal to the detuning $\triangle$. The amplitude of the oscillations increases when increasing E_1^i. At the same time, the power in LM_1 gradually increases while the power in LM_2 decreases when increasing E_1^i. LM_2 is completely turned off at $E_1^i = 0.009$. In the orbit diagram of LM_1, we observe a period doubling for $E_1^i = 0.0085$, and eventually, LM_1 locks to the injected light at $E_1^i = 0.011$. When stable locking occurs, the intensity of the CCW mode is larger than the intensity of the CW mode. This intensity distribution is different from the intensity distribution due to the asymmetry in the backscattering coefficients which normally gives a slightly larger intensity in the CW mode (as can be seen in Fig. 2). The change in the intensity distribution between the two directions represents a directional switching in the output of the SRL. This is due to the OI enhancing the direction in which light is injected.[12,23] Finally, when E_1^i reaches a value of 0.13, a Hopf bifurcation is observed leading to oscillations in the CW and in the CCW intensity close to the relaxation oscillation frequency.

Next, we increase the amount of IOF while the SRL is still subjected to OI. We keep the OI on LM_1 with a strength of $E_1^i = 0.02$, and we increase the amount of IOF on LM_2 from $\eta_2 = 0\,ns^{-1}$ to $\eta_2 = 15\,ns^{-1}$ while using $\theta_2 = 0.5\pi$. We plot the corresponding orbit diagrams for LM_1 and LM_2 in Figs. 5(c) and 5(d), respectively. When we increase η_2, there is initially no change: LM_2 remains being switched off while we observe oscillations in the CW and the CCW direction of LM_1. In this region, the carrier density is too low to activate LM_2. However, when η_2 increases, the carrier density level necessary to provide a positive net gain for LM_2 decreases with increasing feedback strength. At $\eta_2 = 4.4\,ns^{-1}$, LM_2 switches on and both directional modes of LM_2 oscillate in time. At this point, the carrier density value associated with the oscillations in LM_1 is sufficient to provide net gain to LM_2. When we further increase η_2, the oscillations in LM_2 grow in amplitude, while the amplitude of the oscillations in LM_1 gradually decreases. At $\eta_2 = 7.6\,ns^{-1}$, the oscillations in LM_1 and LM_2 disappear and we observe a steady output

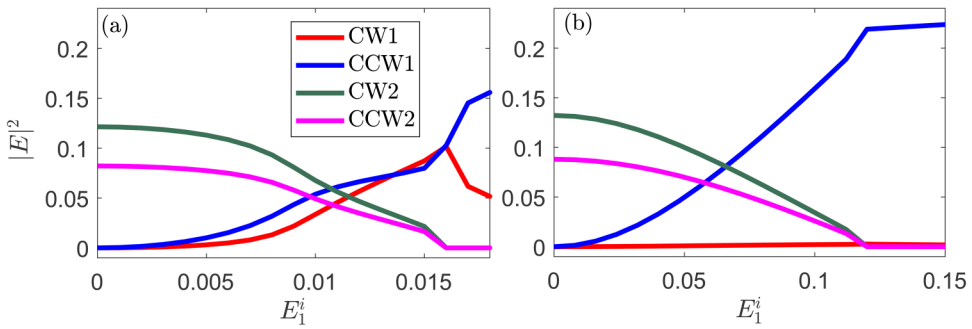

FIG. 6. Field intensity $|E|^2$ as function of the optical injection amplitude using the parameters $\eta_1 = 0\,ns^{-1}$ and $\theta_1 = 0$, $\theta_2 = 0.5\pi$, $\triangle = -4\,ns^{-1}$. (a) $\eta_2 = 4\,ns^{-1}$, (b) $\eta_2 = 15\,ns^{-1}$.

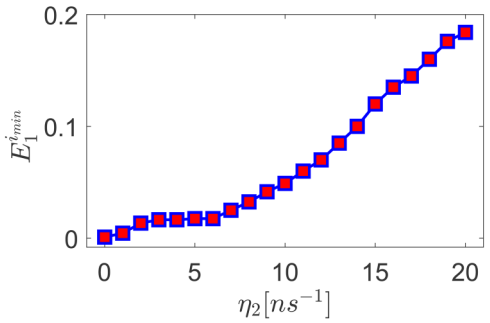

FIG. 7. The minimum amplitude of the OI which is needed to change the output of the laser to LM_1 ($E_1^{i_{min}}$) as a function of the strength of the feedback while $\theta_2 = 0.5\pi$ and the detuning $\triangle = -4\,ns^{-1}$.

intensity in all modes and in both directions. Further increasing η_2 leads to a gradual decrease of LM_1 accompanied by a gradual increase in LM_2. LM_2 now is dominant due to the effect of the IOF, and it is stable even in the presence of OI. It is also clear that the intensity of LM_2 in the CW direction is larger than the one in CCW direction for large values of η_2. This difference is due to the asymmetry in the backscattering coefficients which has been discussed in Fig. 2. These results show that the IOF can suppress the effects of OI. In Secs. IV A–IV D, we investigate the effect of the different parameters of the OI and the IOF on the output of the SRL.

A. Effect of the strength of the OI

We study the role of the strength of the OI in determining the dominant mode of the SRL under the simultaneous effect of OI and IOF. We fix the strength and phase of the IOF by setting $\eta_2 = 4\,ns^{-1}$ and $\theta_2 = 0.5\pi$, then we simulate the laser's output while the strength of OI is increased. We calculate the field intensity $|E|^2$ of the two LMs in the two directions as a function of the optical injection amplitude E_1^i. The results are shown in Fig. 6(a). Remark that during the simulations of Fig. 6, we did not observe oscillations in the intensity, and therefore we only plot in Fig. 6 the steady state solutions. Also remark that in Fig. 6, the IOF is always on, which was not the case in Figs. 5(a) and 5(b). LM_2 is dominant when $E_1^i < 0.0108$ due to the IOF. When increasing E_1^i, we observe a gradual decrease of the power in LM_2 while the power in LM_1 increases. LM_1 and LM_2 have roughly the same intensity when $E_1^i = 0.0108$. Finally, when $E_1^i > 0.0108$, LM_1 is dominant. We consider the minimum injected amplitude $E_1^{i_{min}}$ which is needed to change the output of the laser to LM_1 as the injection strength at which intensity of LM_2 becomes equal to zero. Figure 6(a) then yields $E_1^{i_{min}} = 0.016$. It is worth to mention that if the OI signal is injected to the CW direction instead of the CCW, the OI will enhance the intensity LM_1 in the CW (instead of the CCW).

Next, we repeat the same calculations but this time for a higher IOF strength applied to LM_2 ($\eta_2 = 15\,ns^{-1}$). In this case, the mode which is enhanced by the IOF (LM_2) is still dominant for larger values of OI as can be seen in Fig. 6(b): $E_1^{i_{min}}$ is increased to 0.12, which is 7.5 times larger than the value corresponding to an IOF strength of $\eta_2 = 4\,ns^{-1}$. So increasing η_2 increases the strength of optical injection required to switch the laser output to LM_1.

We notice in the two panels of Fig. 6 that when the mode which is enhanced by OI (LM_1) is dominant, the intensity distribution between the two directions is different from the intensity distribution between the two directions due to the asymmetry in the backscattering coefficients. This observation is more pronounced in Fig. 6(b), where the intensity of LM_1 in the CW direction is decreased to zero.

B. Effect of the strength of the IOF on the SRL with OI

We quantify the role of the IOF by investigating the minimum amplitude of the OI signal needed to change the output of the laser to LM_1 ($E_1^{i_{min}}$) as a function of the strength of the feedback while $\theta_2 = 0.5\pi$. The results are shown in Fig. 7 where it can be seen that $E_1^{i_{min}}$ increases when increasing the applied feedback. This result can be understood due to the fact that increasing the strength of the IOF will increase the effective strength of LM_2. This requires a larger external OI to change the laser's output from LM_2 to LM_1. The dominant LM is thus determined according to the competition between the LM which is enhanced by the IOF and the LM which is enhanced by OI.

C. Effect of the phase of the IOF on the SRL with OI

We study the role of the phase of the IOF in determining the dominant mode of the SRL under the effect of OI and IOF simultaneously. We use a fixed feedback strength $\eta_2 = 10\,ns^{-1}$ and detuning $\triangle = -5\,ns^{-1}$. Then we calculate $E_1^{i_{min}}$ for different values of θ_2 in the range [0–2π]. The results are shown in Fig. 8(a) where we notice that $E_1^{i_{min}}$ is dependent on the phase θ_2 of IOF. When the phase is in the range [0π–0.6π], or in the range [1.2π–2.0π], $E_1^{i_{min}}$ decreases when increasing the phase (θ_2). This shows, as was also noticed in the discussion of Fig. 2(b), that the phase of the

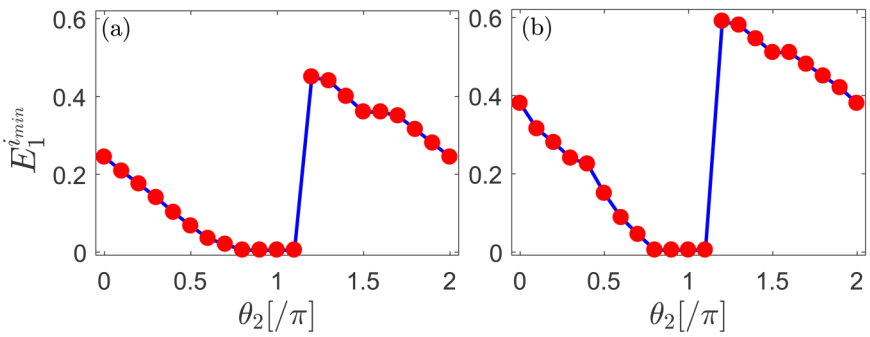

FIG. 8. The minimum amplitude of the OI which is needed to change the output of the laser to LM_1 ($E_1^{i_{min}}$) as a function of the phase of the feedback while $\eta_2 = 10\,ns^{-1}$ and the detuning (a) $\triangle = -5\,ns^{-1}$, (b) $\triangle = 5\,ns^{-1}$.

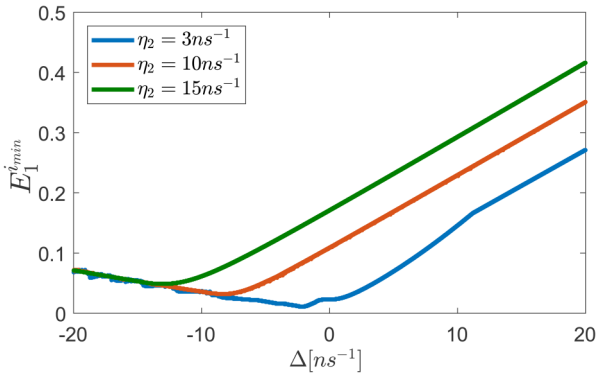

FIG. 9. The minimum amplitude of the OI which is needed to change the output of the laser to LM_1 ($E_1^{i_{min}}$) as a function of the detuning while $\theta_2 = 0.5\pi$ and $\eta_2 = 3\,ns^{-1}$, $\eta_2 = 10\,ns^{-1}$, and $\eta_2 = 15\,ns^{-1}$.

IOF changes its effective strength. In the range $[0.7\pi$–$1.1\pi]$, $E_1^{i_{min}}$ is very small (0.005) as the phase of the IOF favors LM_1 (as has been shown in Sec. III) which is also preferred by the OI.

We repeat the calculations using a detuning with different sign ($\triangle = 5\,ns^{-1}$). The results are shown in Fig. 8(b), which is very similar to the graph for $\triangle = -5\,ns^{-1}$. These results show the importance of controlling the phase of the IOF. This can be achieved easily in an integrated device using a phase shifter section.[26]

D. Effect of the detuning between the OI and the closest LM of the SRL

Here, we investigate the effect of the detuning (between the OI signal and one of the LMs of the SRL) on the stability of the SRL. We start by calculating the minimum amplitude of the OI ($E_1^{i_{min}}$) which is needed to change the output of the laser to LM_1 for the different values of the detuning $\triangle$ in the range $[-20$ to $20]\,ns^{-1}$. We perform the simulations using the same parameters as in Sec. IV C and for three values of the strength of the IOF ($3\,ns^{-1}$, $10\,ns^{-1}$, and $15\,ns^{-1}$) while the phase of the IOF is fixed to $\theta_2 = 0.5\pi$. The results of the simulations are shown in Fig. 9, where we can notice that $E_1^{i_{min}}$ depends on the strength of the IOF.

Starting from $\triangle = -20\,ns^{-1}$, we first see that $E_1^{i_{min}}$ decreases when $\triangle$ increases. Then, the $E_1^{i_{min}}$ locking curves go through a minimum, after which $E_1^{i_{min}}$ increases for increasing values of $\triangle$. For low negative values of $\triangle$, the curves corresponding to different values of the IOF strength overlap, but the minimum of locking curve is clearly dependent on the value of η_2. As a result, there is a large difference in $E_1^{i_{min}}$ for larger values of $\triangle$. The $E_1^{i_{min}}$ curves of Fig. 9 look similar to typical injection locking curves when the injection happens close to the free-running mode (instead of a side-mode), but there are some important changes visible in Fig. 9. The minimum of the locking curve does not happen at detuning $\triangle = 0\,ns^{-1}$, but this minimum is shifted to negative values of the detuning. The magnitude of this shift depends on the strength η_2 of the IOF. This shift of the locking curve's minimum goes together with an increase of the value of $E_1^{i_{min}}$ at the minimum. We can, therefore, conclude that the effects of OI can be suppressed by increasing the strength of the IOF.

It is also clear from Fig. 9 that $E_1^{i_{min}}$ is generally larger for positive values of $\triangle$ than for negative values. This asymmetric sensitivity to the injection strength with respect to detuning has been reported in different studies.[9,10,45–49] In some studies, it has been attributed to the shift of the gain peak toward longer wavelengths under the effect of optical injection. However, in our case, we think it is more likely to be an alpha-parameter induced effect.[45,46]

V. CONCLUSIONS

We have numerically studied the behavior of an SRL under the simultaneous effect of IOF and OI. When IOF is applied selectively to one mode, the minimum in the side-mode injection locking curve shifts to more negative values of the detuning between the injection signal and the side-mode. At the same time, the minimum in the locking curve increases. We have thus shown that IOF can be used to reduce the effects of the external OI: the IOF results in an increase of the strength of the OI that is required to change the laser's emission wavelength and directional power distribution. Decreasing the sensitivity of semiconductor lasers to external optical injection using IOF will be an added value for these lasers in lot of applications in which unintentional OI should be avoided or suppressed.

ACKNOWLEDGMENTS

The authors acknowledge the Research Foundation Flanders (FWO), Hercules Foundation, and Research Council of the VUB. M.K. wishes to acknowledge partial financial support by FWO by way of EOS Project No. G0F6218N (EOS ID 30467715).

[1]G. H. M. Van Tartwijk and D. Lenstra, "Semiconductor lasers with optical injection and feedback," Quantum Semiclass. Opt. **7**, 87–143 (1995).
[2]R. Lang, "Injection locking properties of a semiconductor laser," IEEE J. Quantum Electron. **18**, 976–983 (1982).
[3]F. Mogensen, H. Olesen, and G. Jacobsen, "FM noise suppression and linewidth reduction in an injection-locked semiconductor laser," Electron. Lett. **21**, 696–697 (1985).
[4]C. R. Mirasso, P. Colet, and P. Garcia-Fernandez, "Synchronization of chaotic semiconductor lasers: Application to encoded communications," IEEE Photon. Technol. Lett. **8**, 299–301 (1996).
[5]S. Osborne, P. Heinricht, N. Brandonisio, A. Amann, and S. O'Brien, "Wavelength switching dynamics of two-colour semiconductor lasers with optical injection and feedback," Semicond. Sci. Technol. **27**, 094001 (2012).
[6]J. Wang, M. K. Halder, L. Li, and F. V. C. Mendis, "Enhancement of modulation bandwidth of laser diodes by injection locking," IEEE Photon. Technol. Lett. **8**, 34–36 (1996).
[7]J. M. Liu, H. F. Chen, X. J. Meng, and T. B. Simpson, "Modulation bandwidth, noise, and stability of a semiconductor laser subject to strong injection locking," IEEE Photon. Technol. Lett. **9**, 1325–1327 (1997).
[8]T. B. Simpson, J. M. Liu, and A. Gavrielides, "Small-signal analysis of modulation characteristics in a semiconductor laser subject to strong optical injection," IEEE J. Quantum Electron. **32**, 1456–1468 (1996).
[9]L. Goldberg, H. F. Taylor, and J. F. Weller, "Intermodal injection locking of semiconductor lasers," Electron. Lett. **20**, 809–811 (1984).
[10]J. M. Luo and M. Osinski, "Stable-locking bandwidth in sidemode injection locked semiconductor lasers," Electron. Lett. **27**, 1737–1739 (1991).
[11]G. Yuan, X. Zhang, and Z. Wang, "Chaos generation in a semiconductor ring laser with an optical injection," Optik **124**, 5715–57158 (2013).
[12]G. Yuan and S. Yu, "Bistability and switching properties of semiconductor ring lasers with external optical injection," IEEE J. Quantum Electron. **44**, 41–48 (2008).

[13]L. Bi, "On-chip optical isolation in monolithically integrated nonreciprocal optical resonators," Nat. Photon. **5**, 758–762 (2011).
[14]T. Shintaku, "Integrated optical isolator based on efficient nonreciprocal radiation mode conversion," Appl. Phys. Lett. **73**, 1946–1948 (1998).
[15]M. C. Tien, T. Mizumoto, P. Pintus, H. Kromer, and J. E. Bowers, "Silicon ring isolators with bonded nonreciprocal magneto-optic garnets," Opt. Express **19**, 11740–11745 (2011).
[16]L. Sun, S. Jiang, J. D. Zuegel, and J. R. Marciante, "All-fiber optical isolator based on Faraday rotation in highly terbium-doped fiber," Opt. Lett. **35**, 706–708 (2010).
[17]J. Ballato and E. Snitzer, "Fabrication of fibers with high rare-earthconcentrations for Faraday isolator applications," Appl. Opt. **34**, 6848–6854 (1995).
[18]M. Khoder, G. Van der Sande, J. Danckaert, and G. Verschaffelt, "Effect of external optical feedback on tunable micro-ring lasers using on-chip filtered feedback," IEEE Photonics Technol. Lett. **28**, 959–962 (2016).
[19]B. Docter, J. Pozo, S. Beri, I. V. Ermakov, J. Danckaert, M. K. Smit, and F. Karouta, "Discretely tunable laser based on filtered feedback for telecommunication applications," IEEE J. Sel. Top. Quantum Electron. **16**, 1405–1412 (2010).
[20]G. Morthier and P. Mechet, "Theoretical analysis of unidirectional operation and reflection sensitivity of semiconductor ring or disk lasers," IEEE J. Quantum Electron. **49**, 1097–1101 (2013).
[21]M. T. Hill, H. J. S. Dorren, T. de Vries, X. J. M. Leijtens, J. H. den Besten, B. Smalbrugge, Y. S. Oei, H. Binsma, G. D. Khoe, and M. K. Smit, "A fast low-power optical memory based on coupled micro-ring lasers," Nature **432**, 206–209 (2004).
[22]R. M. Nguimdo, G. Verschaffelt, J. Danckaert, X. J. M. Leijtens, J. Bolk, and G. Van der Sande, "Fast random bits generation based on a single chaotic semiconductor ring laser," Opt. Express **20**, 28603–28613 (2012).
[23]L. Gelens, S. Beri, G. Van der Sande, J. Danckaert, N. Calabretta, H. J. S. Dorren, R. Notzel, E. A. J. M. Bente, and M. K. Smit, "Optical injection in semiconductor ring lasers: Backfire dynamics," Opt. Express **16**, 10968–10974 (2008).
[24]N. Calabretta, S. Beri, L. Gelens, R. N. Notzel, E. Bente, J. Danckaert, M. Smit, and H. Dorren, "Experimental investigation of bistable operation of semiconductor ring lasers under optical injection," in *Proc. CLEO/QELS, San Jose* (2008).
[25]W. Coomans, S. Beri, G. Van der Sande, L. Gelens, and J. Danckaert, "Optical injection in semiconductor ring lasers," Phys. Rev. A **20**, 033802 (2010).
[26]G. Verschaffelt, M. Khoder, and G. Van der Sande, "Random number generator based on an integrated laser with on-chip optical feedback," Chaos **27**, 114310 (2017).
[27]M. Khoder, "Longitudinal modes competition in a micro ring laser subject to both a self and a cross optical feedback," Commun. Nonlinear Sci. Numer. Simul. **62**, 146–156 (2018).
[28]G. Verschaffelt and M. Khoder, "Directional power distribution and mode selection in micro ring lasers by controlling the phase and strength of filtered optical feedback," Opt. Express **26**, 14315–14328 (2018).
[29]I. V. Ermakov, S. Beri, M. Ashour, J. Danckaert, B. Docter, J. Bolk, X. J. M. Leijtens, and G. Verschaffelt, "Semiconductor ring laser with on-chip filtered optical feedback for discrete wavelength tuning," IEEE J. Quantum Electron. **48**, 129–136 (2012).
[30]M. Khoder, G. Verschaffelt, R. M. Nguimdo, J. Bolk, X. Leijtens, and J. Danckaert, "Controlled multiwavelength emission using semiconductor ring lasers with on-chip filtered optical feedback," Opt. Lett. **38**, 2608–2610 (2013).
[31]G. Friart, G. Van der Sande, M. Khoder, T. Erneux, and G. Verschaffelt, "Stability of steady and periodic states through the bifurcation bridge mechanism in semiconductor ring lasers subject to optical feedback," Opt. Express **25**, 339–350 (2017).
[32]M. Khoder, G. Verschaffelt, R. M. Nguimdo, J. Bolk, X. Leijtens, and J. Danckaert, "Digitally tunable dual wavelength emission from semiconductor ring lasers with filtered optical feedback," Laser Phys. Lett. **10**, 075804 (2013).
[33]M. Khoder, R. M. Nguimdo, X. Leijtens, J. Bolk, J. Danckaert, and G. Verschaffelt, "Wavelength switching speed in semiconductor ring lasers with on-chip filtered optical feedback," IEEE Photonics Technol. Lett. **26**, 520–523 (2014).
[34]R. El-Ganainy, P. Kumar, and M. Levy, "On-chip optical isolation based on nonreciprocal resonant delocalization effects," Opt. Lett. **38**, 61–63 (2013).
[35]M. Sargent III, "Theory of a multimode quasiequilibrium semiconductor laser," Phys. Rev. A. **48**, 717–726 (1993).
[36]C. Etrich, P. Mandel, N. B. Abraham, and H. Zeghlache, "Dynamics of a two-mode semiconductor laser," IEEE J. Quantum Electron. **28**, 811–821 (1992).
[37]M. Radziunas, M. Khoder, V. Tronciu, J. Danckaert, and G. Verschaffelt, "Semiconductor ring laser with filtered optical feedback: Traveling wave description and experimental validation," J. Opt. Soc. Am. B **35**, 380–390 (2018).
[38]S. T. Kingni, G. Van der Sande, I. V. Ermakov, and J. Danckaert, "Theoretical analysis of semiconductor ring lasers with short and long time-delayed optoelectronic and incoherent feedback," Optics Com. **341**, 147–154 (2015).
[39]M. Sorel, P. J. R Laybourn, A. Scirè, S. Balle, G. Giuliani, R. Miglierina, and S. Donati, "Alternate oscillations in semiconductor ring lasers," Opt. Lett. **27**, 1992–1994 (2002).
[40]M. Sorel, G. Giuliani, A. Scié, R. Miglierina, S. Donati, and P. J. R. Laybourn, "Operating regimes of GaAs-AlGaAs semiconductor ring lasers: Experiment and model," IEEE J. Quantum Electron **39**, 1187–1195 (2003).
[41]R. Lang and K. Kobayashi, "External optical feedback effects on semiconductor injection laser properties," IEEE J. Quantum Electron. **16**, 347–355 (1980).
[42]S. Fürst, S. Yu, and M. Sorel, "Fast and digitally wavelength-tunable semiconductor ring laser using a monolithically integrated distributed Bragg reflector," IEEE Photonics Technol. Lett. **20**, 1926–1928 (2008).
[43]X. Leijtens, "JePPIX: The platform for indium phosphide-based photonics," IET Optoelectron. **5**, 202–206 (2011).
[44]T. Erneux, F. Rogister, A. Gavrielides, and V. Kovanis, "Bifurcation to mixed external cavity mode solutions for semiconductor lasers subject to optical feedback," Opt. Commun. **183**, 467–477 (2000).
[45]A. Bogatov, P. Eliseev, and B. Sverdlov, "Anomalous interaction of spectral modes in a semiconductor laser," IEEE J. Quantum Electron. **11**, 510–515 (1975).
[46]R. Lang, "Injection locking properties of a semiconductor laser," IEEE J. Quantum Electron. **18**, 976–983 (1982).
[47]J. M. Luo and M. Osinski, "Comparison of side-mode and peak-mode injection locking characteristics of semiconductor lasers," in *LEOS '92, IEEE Lasers Electro-Optics Society*, pp. 94–95 (IEEE, 1992).
[48]J. M. Luo, M. Osinski, and J. G. McInerney, "Side-mode injection locking of semiconductor lasers," IEE Proc. J. Optoelectron. **136**, 33–37 (1989).
[49]Y. Hong and K. A. Shore, "Locking characteristics of a side-mode injected semiconductor laser," IEEE J. Quantum Electron. **35**, 1713–1717 (1999).